University of Nevada, Reno

"Magic" Trapping of a Three-Level System for Rydberg Quantum Computation

A thesis submitted in partial fulfillment
of the requirements for the degree of

Bachelor of Science in Physics and the Honors Program

by

Muir J. Morrison

Dr. Andrei Derevianko, Thesis Advisor

May, 2012

UNIVERSITY OF NEVADA RENO

THE HONORS PROGRAM

We recommend that the thesis
prepared under our supervision by

MUIR J. MORRISON

entitled

"Magic" Trapping of a Three-Level System for Rydberg Quantum Computation

be accepted in partial fulfillment of the
requirements for the degree of

BACHELOR OF SCIENCE

Andrei Derevianko, Ph.D., Advisor

Jonathan Weinstein, Ph.D., Committee Member

Andrew Geraci, Ph.D., Committee Member

Tamara Valentine, Ph.D., Director, Honors Program

May, 2012

Abstract

For over a decade, enormous effort has been invested towards building a practical quantum computer. Such a machine promises to revolutionize scientific computing, but there are many challenges to be overcome. The dominant problem for most proposals is decoherence: random and uncontrollable loss of quantum information to the computer's environment. Here we consider one promising implementation for quantum computation using the Rydberg blockade mechanism, which stores qubits in optically trapped neutral atoms. A detailed theory for these optical traps is presented. While the traps are essential, they induce decoherence in the atoms they trap. We propose a method of "magic" trapping by which this decoherence may be completely removed. Numerical calculations show that, while the commonly used alkalis cannot be trapped with this scheme, a "magic" trap could be built for aluminum.

Acknowledgements

I cannot overstate my gratitude to my advisor, Dr. Andrei Derevianko. None of this would have been possible without his encouragement and patient explanations.

I would also like to thank my committee, especially Dr. Jonathan Weinstein for getting me started in scientific research.

I am also grateful for receiving a UNR Honors Undergraduate Research Award for this work.

For helping me keep my sanity the last five years, I cannot thank Rachel enough.

Last but certainly not least, I thank my parents for encouraging my curiosity for as long as I can remember. Their boundless pride in everything I do means the world to me.

Contents

List of Figures

Chapter 1

Introduction

1.1 Motivation for Quantum Computation

Quantum computation was first suggested by Feynman [9]. Noting the inherent inefficiency in simulating quantum phenomena with classical computers, Feynman proposed instead to simulate one quantum system with another. This simulator would be composed of computing elements that obey the laws of quantum, rather than classical, mechanics. Deutsch [7] formalized some implications of this by defining a universal quantum computer, a generalization of a Turing machine, and exploring some basic algorithms that could be performed with such a hypothetical machine. It is worth emphasizing that Deutsch suggests, but does not conclusively demonstrate, that some problems could be solved faster with a quantum computer than with a classical computer.

Such a demonstration was first achieved in Shor's landmark work [23], which provided an efficient algorithm for factoring large integers.[1] In classical complexity theory, this problem is regarded as so difficult[2] that it forms the basis of the widely

[1] Simon's algorithm [24] was developed first and even inspired Shor's algorithm, but it solves a "black box" problem that is of little practical interest.

[2] More precisely, Shor's algorithm is polynomial time: the required computing time is a polynomial function of the size of the input (the number of digits), while the best classical algorithm is super-polynomial (in fact, sub-exponential) and therefore impossibly slow for large numbers.

used RSA encryption system [18].

Since Shor's original work, there has been a proliferation of proposed quantum algorithms which offer significant computational speed-up compared to classical algorithms (see, e.g., reviews [4] and [17]). In short, a practical quantum computer would enable a revolution in the computational sciences.

1.2 Experimental Realization

Following from the theoretical motivations in Sec. 1.1, there have been intense experimental efforts in recent years to build a useful quantum computer (see, e.g., reviews on ions [25], superconductors [5], and atoms [20]). Although their details vary widely, most center around *qubits* (a contraction of *qu*antum *bits*), the quantum analog of 0s and 1s familiar from classical binary computers.

Like classical algorithms, quantum algorithms contain sequences of gate operations to be performed on qubits, usually categorized into one- and two-qubit operations. Unlike classical algorithms, quantum algorithms must make careful consideration of measurement operations as well, since unlike a classical computer, observing a qubit in the middle of a computation usually destroys the result.

Essentially then, paraphrasing DiVincenzo [8], building a useful quantum computer has a few broad requirements:

1. Choose a system to store the qubits with favorable scalability.

2. Implement measurements and gate operations on the qubits.

3. Protect the qubits from decoherence.

The primary outstanding challenges are scalability (increasing the number of qubits) and decoherence (irreversible loss of a qubit's information to its environment).

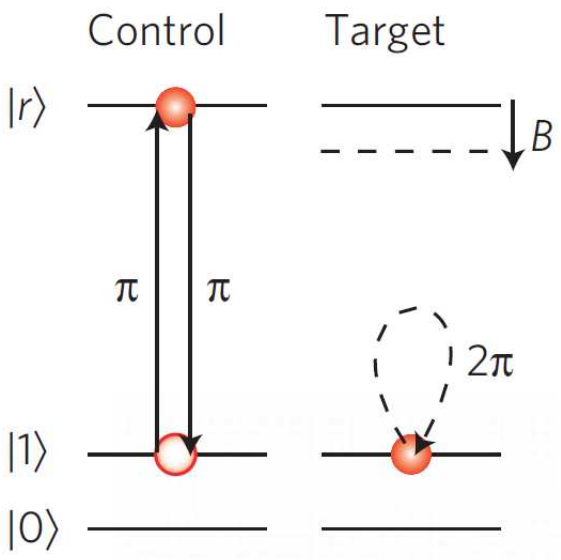

Figure 1.1: (Color online) Relevant energy levels in the Rydberg blockade scheme. Qubits $|0\rangle$ and $|1\rangle$ are stored in hyperfine sublevels of the ground state in each atom. Interactions are turned on when the control atom is excited to a Rydberg state $|R\rangle$ (π pulses), accompanied by a shift B of its neighbor's energy levels. Adapted from Ref. [26]

This thesis focuses on one particular implementation of quantum computing, outlined below in Sec. 1.3.

1.3 Rydberg blockade

The Rydberg blockade implementation of quantum computing was originally proposed by Jaksch *et. al.* [11]. In this scheme, a single qubit is stored in an atom's internal energy levels (usually two hyperfine sublevels attached to the ground state). Gate operations are achieved through highly excited Rydberg states. Fig. 1.1 depicts the level structure.

To illustrate the method, we outline an experimental implementation demonstrated in [26]. Multiple atoms are trapped near each other using optical traps, discussed in detail in Chap. 2. Laser pulses control two-qubit gate operations on

neighboring atoms by toggling their interaction on and off as follows. Trapped at $\sim \mu m$ separations, neutral ground state atoms have negligible interactions, but Rydberg states with principal quantum number $n \sim 100$ have a spatial extent on the order of a μm. Thus when one atom is excited to the Rydberg state $|R\rangle$, a neighboring atom experiences a strong electric dipole force that shifts its Rydberg levels, which blocks excitation of the second atom to $|R\rangle$. The excitation to $|R\rangle$ is also dependent on the qubit state so that, for instance, $|1\rangle$ can be excited to $|R\rangle$ but $|0\rangle$ can not be excited. With such a protocol, blockade interactions can be used to entangle the atoms and execute CNOT gates, forming a basis for arbitrary logic gates in the circuit model of quantum computation.[3]

Basic qubit operations have been experimentally demonstrated using the Rydberg blockade [26], and their fidelity is improving [21]. While some technical issues remain in order to improve the gate operations [21], the Rydberg blockade holds great potential for scaling to a large number of qubits. A variety of methods for doing so are surveyed in [20].

This thesis is concerned with the optical traps used in these experiments, and in particular, two problems arising from the traps: atom loss and decoherence. In experiments thus far, the ground and Rydberg states experience vastly different potentials due to the laser trap, so the laser trap must be turned off when an atom is excited to a Rydberg state.[4] The atom may or may not be successfully recaptured when the trap is turned back on after de-excitation. Moreover, even if the atom is recaptured, the qubit's information is now entangled with the atom's center of mass motion, leading to decoherence [20]. Either outcome reduces gate fidelity. Furthermore, in between

[3]Proposals exist [20] for controlling interactions between widely separated atoms in an array, or for using mesoscopic ensembles of atoms [12], but the blockade interaction remains essentially the same.

[4]In fact, for the widely-used red-detuned traps, the ground state potential is attractive while the excited state potential is repulsive. Chap. 2 contains more details. Also, photoionization of the Rydberg state is a problem in red-detuned traps [26].

gate operations, the trap can directly induce qubit decoherence since the qubit states have a different trapping potential. This motivates the development of a new type of trap that can remain on while the atom is excited to a Rydberg level.

These requirements are quite similar to those for optical lattice clocks. In clock experiments, the critical quantity is the energy spacing between two levels. Time is defined in terms of the frequency of photons emitted or absorbed when the atom undergoes a transition between the two levels. Therefore, any effect that disturbs the energy splitting leads to clock errors; in particular, the trapping laser itself shifts the levels significantly. The solution is known as a "magic" trap (see, e.g., [15, 28]) in which a particular laser wavelength is chosen such that the two clock states experience the same shift. This means the internal and external degrees of freedom of the atom are completely decoupled, if we are only interested in these two states.

For the present problem, we have three, not two, levels for which we must build a magic trap: a Rydberg state along with two qubit states.

This thesis contains a theoretical proposal, supported by computational results, for reducing decoherence in the Rydberg blockade implementation of quantum computation. Chapter 2 considers the Stark-effect formalism necessary to describe optical trapping of atoms and introduces the concept of "magic" optical trapping. Chapter 3 presents computational results for several atomic species, and Appendix A outlines our library of atomic structure computer codes.

Chapter 2

"Magic" optical traps and Stark-effect theory

2.1 Optical traps

Before giving a quantitative treatment of optical trapping of atoms, we offer some classical intuition. When an atom is placed in an electric field, the field polarizes the atom, pulling the electrons and protons in opposite directions. This creates an electric dipole which can then interact with the field; in particular, if the field is non-uniform, there will be a net force on the atom, which can be used to trap the atom with appropriately chosen geometry.[1]

Quantum mechanically, the interaction of an atom with an external electric field is described by the Stark effect. Consider an atom in some state $|nF, M_F\rangle$ with total angular momentum F, projection M_F, and any additional quantum numbers necessary to describe the state collectively denoted n. The atom experiences an energy shift δE_{nFM_F} proportional to the square of the electric field $\mathcal{E}$, given by[2]

$$\delta E_{nFM_F} = -\alpha^{tot}_{nFM_F} \left(\frac{\mathcal{E}}{2}\right)^2, \tag{2.1}$$

[1] This argument applies to any polarizable dielectric; it has even been used to trap μm size scale glass beads [].

[2] Eq. (2.1) is the quadratic (in $\mathcal{E}$) Stark effect. There also exists a *linear* Stark effect if the atom has degenerate states of opposite parity, but no such states appear in this thesis.

where $\alpha^{tot}_{nFM_F}$ is known as the polarizability, discussed in detail in Sec. 2.2. Briefly, $\alpha^{tot}_{nFM_F}$ depends only on the atom's internal energy level structure,[3] so it may be regarded as a constant.

We can now see why optical trapping is possible using non-uniform electric fields generated by laser beams. Consider first the case in which $\alpha^{tot}_{nFM_F} > 0$, commonly called a red-detuned trap[4]. Then the energy is minimized when the atom is at a location of maximum field intensity. This creates an attractive potential, drawing the atom towards a high-intensity location, which effectively traps the atom.[5] Fig. 2.1 depicts a realization of such a trap formed by a tightly focused laser beam: the intensity is a maximum at the center of the beam waist and falls off smoothly in all directions, creating an (approximately) harmonic trapping potential.

The case of $\alpha^{tot}_{nFM_F} < 0$ (commonly, blue-detuned) is more difficult to realize experimentally, but also more useful (see, e.g., [20] for a review). In this situation, the atom is attracted to regions of minimum laser intensity, meaning a "barricade" of light must be erected around the atom. One such configuration, dubbed a bottle beam trap, was experimentally demonstrated with Cs atoms [10] and is depicted in Fig. 2.2. This design uses two coaxial laser beams, each with a Gaussian profile but with different beam waists. Interference creates an intensity null at their common focus, surrounded by non-zero laser intensity in all directions.

[3]This is not quite correct and will be clarified in Sec. 2.2. The key point is that $\alpha^{tot}_{nFM_F}$ has no dependence on $\mathcal{E}$, the magnitude of the external electric field.

[4]For reasons discussed in Sec. 2.2, this case occurs when the laser wavelength is set somewhat longer (redder) than a strong atomic transition. Conversely, the case $\alpha^{tot}_{nFM_F} < 0$ is usually called blue-detuned.

[5]The energy shift due to the trap must be large compared to any other forces acting on the atom, such as collisions with other atoms or gravity.

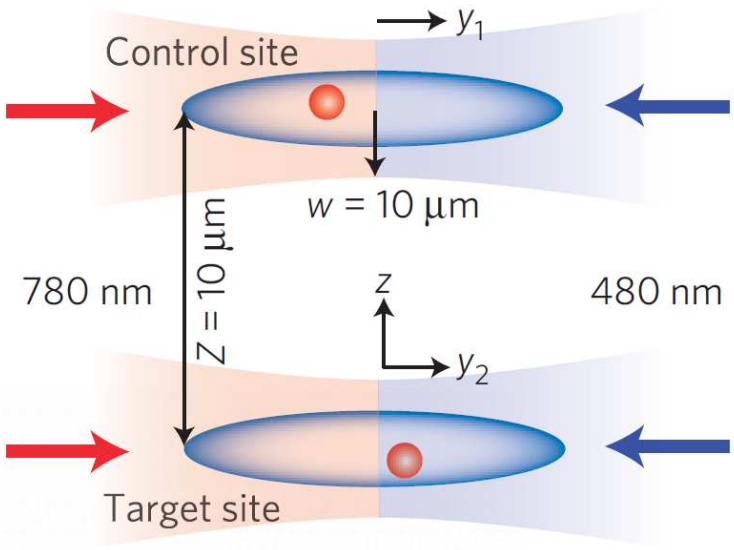

Figure 2.1: (Color online) A red-detuned optical trap may be formed by a tightly focused laser beam. Since $\alpha^{tot}_{nFM_F} > 0$, the atom's potential energy is minimized at the intensity maximum at the center. From Ref. [26].

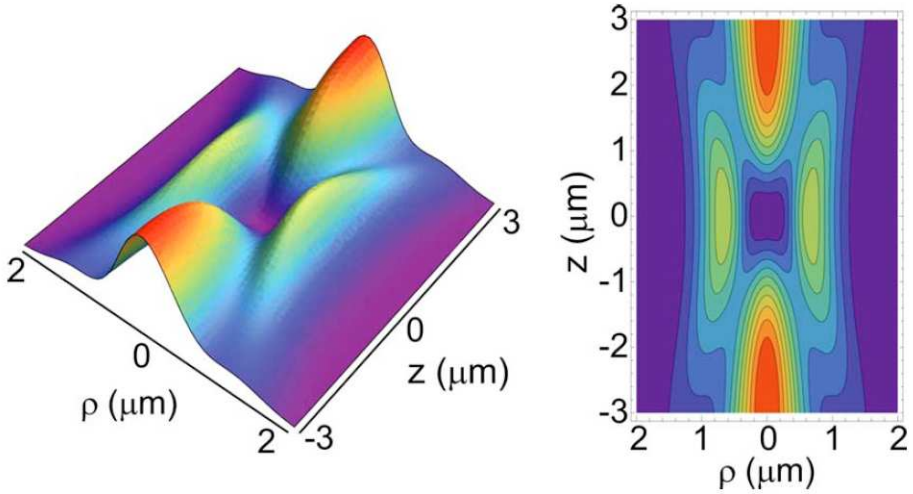

Figure 2.2: (Color online) A blue-detuned optical trap may be formed by the interference of two coaxial laser beams focused to different beam waists. By setting an appropriate relative phase between the two beams, destructive interference is achieved at the trap center. Since $\alpha^{tot}_{nFM_F} < 0$, the atom's potential energy is a minimum at the intensity null at the center. From Ref. [10].

2.1.1 "Magic" Optical Traps

We emphasize that two different atomic states usually have different polarizabilities, i.e., the polarizabilities $\alpha^{tot}_{nFM_F}(\omega)$ and $\alpha^{tot}_{n'F'M_{F'}}(\omega)$ of two states $|nF, M_F\rangle$ and $|n'F', M_{F'}\rangle$, respectively, are generally not equal. This is the cause of the decoherence discussed in Sec. 1.3. When an atom makes a transition from $|1\rangle$ to $|R\rangle$, its trapping potential abruptly changes due to the new polarizability, which can excite vibrational motion of the atom. This remains a problem even if the trap is turned off during Rydberg excitation: no potential is just as detrimental as a different potential. Suppose the atom is initialized in a qubit superposition such as $\frac{1}{\sqrt{2}}(|0\rangle + |1\rangle)$. Following Sec. 1.3, only $|1\rangle$ may be excited to $|R\rangle$, and if this excitation is accompanied by vibrational excitation, the qubit's state becomes entangled with the atom's vibrational state in a random and uncontrollable manner, leading to decoherence. A more formal argument of this point is given in [20].

Conversely, if it happens that the polarizabilities $\alpha^{tot}_{nFM_F}(\omega)$ and $\alpha^{tot}_{n'F'M_{F'}}(\omega)$ are equal, the atom's center of mass motion is completely unaffected by excitation of the atom from $|nF, M_F\rangle$ to $|n'F', M_{F'}\rangle$. This is the precise condition for a "magic" trap introduced in Sec. 1.3: if the polarizabilities are equal, the states' energy splitting is constant, regardless of the atom's motion in the trap. This also removes qubit decoherence induced directly from the trap, since the qubits' splitting determines how phase evolves for a superposition.

Thus, our goal is to theoretically determine "magic" trapping conditions that match polarizabilities of $|0\rangle$, $|1\rangle$, and $|R\rangle$ simultaneously. To do this, we first present the detailed theory of the Stark effect in Sec. 2.2 below.

2.2 Stark effect theory

2.2.1 Non-magnetic states

Here we summarize the standard ac Stark effect formalism. The treatment is similar to Refs. [13, 16, 19]. Consider an electromagnetic plane wave[6]

$$\vec{\mathcal{E}} = \frac{1}{2}\mathcal{E}\hat{\varepsilon}e^{-i(\vec{k}\cdot\vec{r}-\omega t)} + c.c. \tag{2.2}$$

interacting with an atom. $\mathcal{E}$ is the electric field magnitude, $\hat{\varepsilon}$ is the polarization unit vector, and *c.c.* stands for the complex conjugate of the prior term.[7] In the dipole approximation, the interaction with an atom is

$$V(t) = -\vec{\mathcal{E}}\cdot\mathbf{D} = -\frac{1}{2}\mathcal{E}(\hat{\varepsilon}\cdot\mathbf{D})e^{-i\omega t} + H.c. \tag{2.3}$$

where $\mathbf{D}$ is the atomic electric dipole operator and *H.c.* represents the Hermitian conjugate of the preceding term. We treat this interaction perturbatively using the Floquet formalism used in [19]. This reduces to a problem nearly identical in appearance to standard time-*in*dependent perturbation theory.[8] For instance, the second order energy shift for a state $|n\rangle$ is given by

$$\delta E_n^{[2]} = \sum_{n'} \frac{\langle n|v|n'\rangle\langle n'|v|n\rangle}{E_n - (E_{n'} - \omega)} + \sum_{n'} \frac{\langle n|v|n'\rangle\langle n'|v|n\rangle}{E_n - (E_{n'} + \omega)} \tag{2.4}$$

where $v = -\frac{1}{2}\mathcal{E}(\hat{\varepsilon}\cdot\mathbf{D})$, and additional quantum numbers have been suppressed for clarity. Note the sum over intermediate states n' includes all bound states of the atom, as well as unbound continuum states. This point is critical for our numerical

[6] We use atomic units throughout unless noted otherwise.
[7] The effect of the magnetic portion of the light is negligible at our level of approximation.
[8] See [1] for an excellent discussion of this procedure.

calculations, discussed in Appendix A.

Eq. (2.4) may be reduced to a more useful form in terms of irreducible tensor operators. The details may be found in [19]. Ultimately, one finds that the ac Stark shift of a state $|nF, M_F\rangle$ with total angular momentum[9] $\vec{F} = \vec{J} + \vec{I}$ and projection M_F can be written as

$$\delta E_{nFM_F} = -\left(\frac{\mathcal{E}}{2}\right)^2 \left[\alpha^S_{nF}(\omega) + (\hat{k}\cdot\hat{B})\,\mathcal{A}\,\frac{M_F}{2F}\alpha^a_{nF}(\omega) + \frac{1}{2}\left(3|\hat{\varepsilon}\cdot\hat{B}|^2 - 1\right)\frac{3{M_F}^2 - F(F+1)}{F(2F-1)}\alpha^T_{nF}(\omega)\right]. \quad (2.5)$$

$\mathcal{A}$ is the degree of circular polarization ($|\mathcal{A}| \leq 1$), while α^S_{nF}, α^a_{nF}, and α^T_{nF} are the irreducible scalar, vector, and tensor polarizabilities, respectively.[10] The polarizabilities contain expressions resembling Eq. (2.4), but they are much easier to evaluate. Note also that the polarizabilites depend on the light frequency ω, but otherwise depend only on the atom's internal structure. Conveniently, the dependence on field strength $\mathcal{E}$ has been factored out as well. The quantity in square brackets is the total polarizabiltiy, denoted $\alpha^{tot}_{nFM_F}$, in which case we recover Eq. (2.1).

The unit vectors in Eq. (2.5) are the laser wavevector ($\hat{k}$), laser polarization ($\hat{\varepsilon}$), and bias magnetic field ($\hat{B}$). Their relative geometry is shown in Fig. 2.3. The bias magnetic field is a static, externally applied field which defines the quantization axis by breaking the Zeeman degeneracy. This "quantizing magnetic field" guarantees that M_F remains a "good" quantum number for the ac Stark effect perturbation formalism, from which Eq. (2.5) follows.[11] For linearly polarized light, $\hat{\varepsilon}\cdot\hat{B} = \cos\theta_p$, where θ_p is the angle between the polarization and quantization unit vectors. If we

[9] J and I are the total electronic and nuclear spin angular momenta, respectively.

[10] Eq. (2.5) only contains the diagonal matrix elements of the polarizability operator; usually the off-diagonal matrix elements can be neglected, but they will be important in Sec. 2.2.2.

[11] The energy shifts caused by the Stark effect must be small compared to the Zeeman splitting of the magnetic sublevels.

consider circularly polarized light, defining $\hat{\varepsilon}$ using Jones calculus conventions, then $\left|\hat{\varepsilon}\cdot\hat{B}\right|^2 = \frac{1}{2}\sin^2\theta_k$, where θ_k is the angle between the wavevector and quantization unit vectors.

With Eq. (2.5) we can precisely state our goal for "magic" trapping: we must find ω and either θ_k or θ_p such that the Rydberg polarizability $\alpha_{Ryd}(\omega,\theta)$ and the qubit state polarizabilities $\alpha_{nFM_F}(\omega,\theta)$ and $\alpha_{nF'M_{F'}}(\omega,\theta)$ are all equal. The polarizabilities in Eqs. (2.1) and (2.5) may be the conventional second-order quantities, as in Eq. (2.4) and [13], or they may be replaced with third-order hyperfine mediated polarizabilities, denoted β and described in detail in [19]. The second-order $\alpha^{tot}_{nFM_F}$ includes only the interaction with the external electric field, ignoring the hyperfine interaction. This accuracy is sufficient for matching Rydberg and ground state polarizabilities, but it cannot produce "magic" conditions for the qubit levels. Without the hyperfine interaction, the qubit levels are degenerate and always experience the same shift, so trivially "magic" conditions result from any choice of ω and θ [19]. A complete treatment of the qubit states must proceed to third-order perturbation theory, including hyperfine and external electric field interactions.

Unfortunately, as we show in Chapter 3, the experimentally convenient alkali metals cannot be "magically" trapped using the above formalism. We next consider magnetic states, including effects neglected above.

2.2.2 Magnetic states

In this section we outline a method to find "magic" conditions for qubit states with nonzero M_F projection, which closely follows the treatment in [6]. The method developed above is not sufficient to find "magic" conditions for the qubit transition in alkalis. Ref. [19] showed that "magic" conditions do not exist for nonmagnetic hyper-

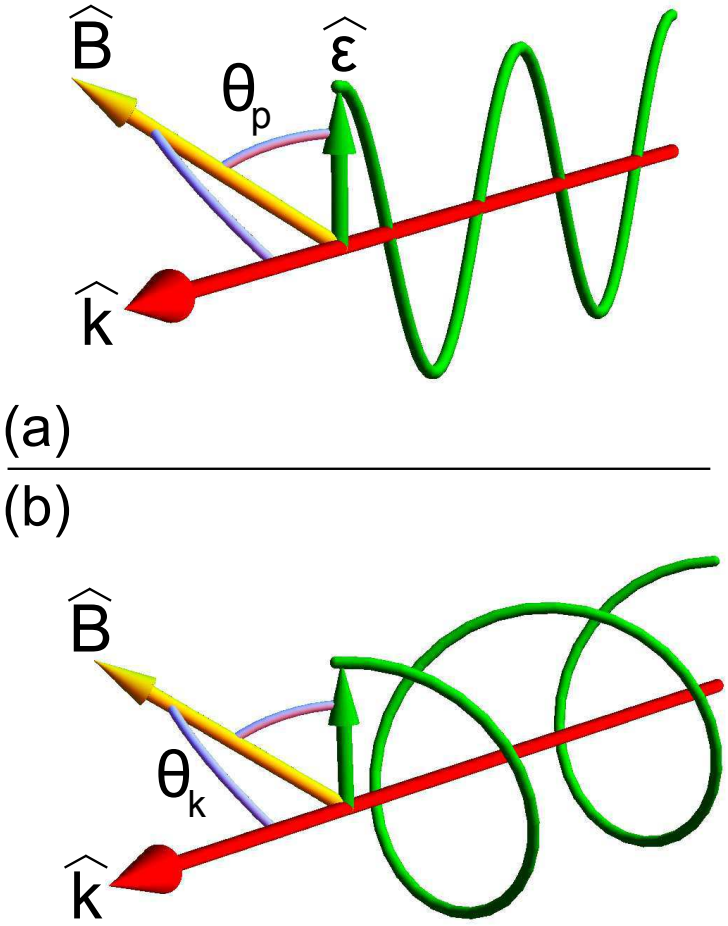

Figure 2.3: (Color online) Relation of angles to unit vectors in Eq. (2.5). (a) For linear polarization, $\hat{k}$, $\hat{\varepsilon}$, and $\hat{B}$ are the laser wavevector, laser polarization, and quantization axis, respectively. θ_p is the angle between the polarization and the quantization axis, defined by the magnetic field. (b) For circular polarization, the relevant angle is θ_k, the angle between the wavevector and the magnetic field. (θ_p is no longer well-defined as $\hat{\varepsilon}$ is time-dependent).

fine states. This is due to the smallness of α^T in comparison with α^S,[12] along with the strict proportionality of $\alpha^S_{nF'M_{F'}}$ and $\alpha^S_{nFM_F}$. However, magnetic substates (with $M_F \neq 0$) have unacceptable Zeeman sensitivity.

A solution to this problem was developed in [6]. Atoms with a $J = 1/2$ ground state are held in a circularly polarized trap to take advantage of vector polarizabilities. States with opposite projections of M_F (i.e., $|nF', M_F\rangle$ and $|nF, -M_F\rangle$) have equal and opposite electronic g-factors[13]. For multiphoton transitions between these states, most of the first order Zeeman shift vanishes. The residual first-order shift is due only to the (much smaller) nuclear magnetic moment, which can be made to cancel the second-order shift with the application of a static magnetic field. The "magic" value of the B-field is given by

$$B_m \approx \frac{g_I \mu_N \; M_{F'}}{2\left|\langle nF, M_{F'}\left|\mu_z^e\right|nF', M_{F'}\rangle\right|^2}\,\omega_{\text{qubit}}\,, \tag{2.6}$$

where ω_{qubit} is the energy splitting between the qubit (hyperfine) levels. While this expression for B_m is only accurate to second-order, it agrees well with the exact analysis [6].

With Zeeman sensitivity removed, we focus on the Stark shift due to the trapping lasers. The relative shift between the qubit states must vanish, i.e., both states must experience the same shift. This condition holds when [6]

$$\begin{aligned}(\beta^s_{nF'} - \beta^s_{nF}) + \delta\beta^T + \mathcal{A}\cos\theta_k \; M_{F'} \\ \times\left[\left(\frac{1}{2F'}\beta^a_{nF'} + \frac{1}{2F}\beta^a_{nF}\right) + g_I\frac{\mu_N}{\mu_B}\left(\frac{B}{B_m}\right)\;\overline{\alpha}^a_{nl_{1/2}}\right] = 0.\end{aligned} \tag{2.7}$$

β^S, β^a, and β^T are the third-order hyperfine mediated polarizabilities referred

[12] From Eq. (2.5), α^a does not enter into α^{tot} for states with $M_F = 0$.
[13] Since $J = 1/2$, there are only 2 hyperfine states, and $F' = F + 1$.

to above, while $\overline{\alpha}^a_{nl_{1/2}}$ is the conventional second-order polarizability.[14] $\delta\beta^T$ absorbs lengthy prefactors. The full form is

$$\delta\beta^T = -\beta^T_{nF'}\frac{3M_F^2 - F'(F'+1)}{2F'(2F'-1)} + \beta^T_{nF}\frac{3M_F^2 - F(F+1)}{2F(2F-1)}. \tag{2.8}$$

B_m is determined from Eq. (2.6), while B is the actual applied field. Ideally $B = B_m$, but as suggested in [6] this is not always possible.

Let us consider Eq. (2.7) qualitatively. As in Sec. 2.2.1, we need the leading-order polarizabilites to cancel, hence the differences of β^S, β^a, and β^T.[15] However, the form of the last term involving $\overline{\alpha}^a_{nl_{1/2}}$ may be surprising. It arises due to interference between the Zeeman shift and the vector part of the Stark shift, as these are both (axial) vector operators [6]. Even though $\mu_N \ll \mu_B$, $\overline{\alpha}^a_{nl_{1/2}} \gg \beta^T_{nF}$, so this term is of a comparable order of magnitude to the rest and must be included in Eq. (2.7).

[14] Note $\overline{\alpha}^a_{nl_{1/2}}$ and α^a_{nF} use different coupling schemes and are not equal.

[15] The apparent sum of β^a is actually a difference due to angular factors hidden inside.

Chapter 3

Results and Conclusions

In this chapter we present results of numerical calculations in search of "magic" optical trapping. Our computer codes are briefly described in App. A. We performed calculations for qubits stored in ground state hyperfine levels in multiple atomic species. The alkalis required the method of Sec. 2.2.2, as discussed therein. For Al, we considered both the methods of Sec. 2.2.1 and Sec. 2.2.2. Before discussing the quantitative results, we outline some generalities.

For Rydberg states, the tensor polarizability is negligible at optical frequencies [13, 22], so the total polarizability is dominated by the scalar part. This follows since the Rydberg electron is barely bound to the atom at all, so it polarizability is essentially equal to that of a free electron, $\alpha^S_{Ryd}(\omega) = -1/\omega^2$. Our *ab initio* calculations confirmed this conclusion; see App. A below for details. Since α^S_{Ryd} is independent of the external fields' geometry (either θ_k or θ_p), the "magic" trap frequency will be determined by $\alpha^S_{Ryd}(\omega) = \alpha^{tot}_{nl_{1/2}}(\omega)$, i.e., when the ground and Rydberg state polarizabilities are equal.

As we show below, evaluating Eq. (2.6) with representative values, we find that B_m is on the order of a few Gauss. This relatively large magnetic field may adversely impact the Rydberg blockade interactions. While a detailed treatment of these effects is well outside the scope of this thesis, the case of Zeeman degenerate blockade states

is considered in [27], and a similar approach should be able to calculate the impact of B_m on the blockade.

3.1 Alkalis

We considered ^{87}Rb first, as it is already in use in experiments [26]. This isotope has nuclear spin $I = 3/2$ and a $J = 1/2$ ground state. The only possible multiphoton transition between the qubit states is from the $|F' = 2, M_{F'} = 1\rangle$ state to the $|F = 1, M_F = -1\rangle$ state, which are attached to the $5s_{1/2}$ electronic ground state. The hyperfine splitting is 6.83 GHz, and from Eq. (2.6), $B_m \approx 3.25$ G.

As noted above, "magic" trapping for the Rydberg states occurs at the ω satisfying $\alpha^S_{Ryd}(\omega) = \alpha^{tot}_{nl_{1/2}}(\omega)$. In Fig. 3.1 we plot α_{Ryd}, $\alpha^S_{5s_{1/2}}$, and the ratio B/B_m. To achieve "magic" trapping for the qubit using the scheme above, we must have $|B/B_m| \leq 1$ in Eq. (2.7). If $|B/B_m|$ is slightly greater than 1, "nearly-magic" trapping is possible as considered in [6]. But in the present case, B/B_m diverges near ω_m, and the B required to remove the Stark shift is prohibitively large. The reason behind this divergence can be seen from Eq. (2.7) by solving for B/B_m:

$$\frac{B}{B_m} = -\frac{\mu_B}{g_I \mu_N \overline{\alpha}^a_{nl_{1/2}}} \left[\frac{(\beta^s_{nF'} - \beta^s_{nF}) + \delta\beta^T}{\mathcal{A} \cos\theta_k \; M_{F'}} + \left(\frac{1}{2F'} \beta^a_{nF'} + \frac{1}{2F} \beta^a_{nF} \right) \right]. \tag{3.1}$$

As B/B_m is inversely proportional to $\alpha^a_{5s_{1/2}}$, this ratio diverges wherever $\alpha^a_{5s_{1/2}}$ is zero.

The situation is qualitatively the same for ^{133}Cs. Our numerical calculations show a similar zero-crossing of $\alpha^a_{6s_{1/2}}$ and corresponding divergence near ω_m. Unfortunately the lighter alkalis have no doubly-magic or nearly-magic points for the qubit transition.

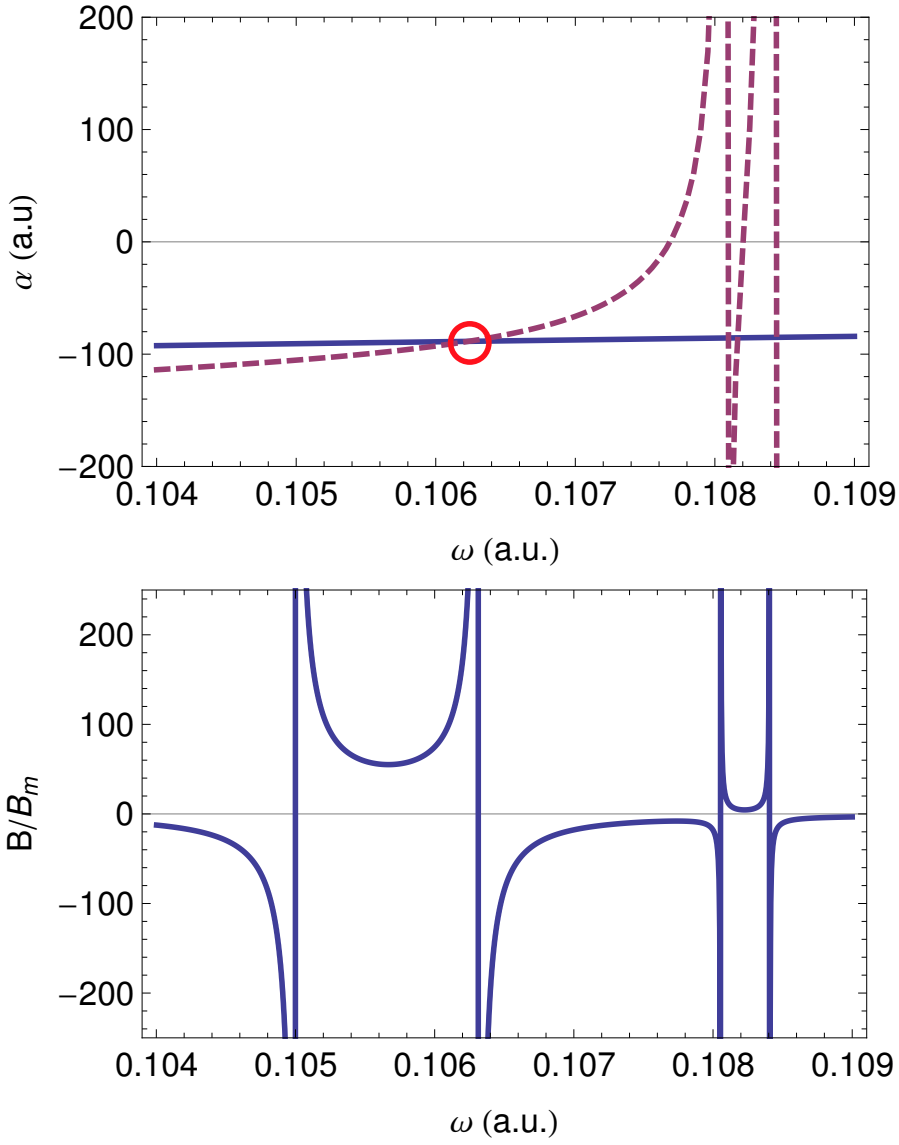

Figure 3.1: (Color online) Polarizabilities of the 5s state (dashed), the Rydberg state (solid), and the ratio B/B_m (lower frame) for the hyperfine transition $|F = 2, M_F = 1\rangle$ to $|F = 1, M_F = -1\rangle$ in ^{87}Rb. Since $\alpha^a_{5s} \ll \alpha^S_{5s}$, the "magic" ω simply occurs where $\alpha_{Ryd} = \alpha^S_{5s_{1/2}}$ at approximately $\omega = 0.1062$ a.u. ($\lambda = 429$ nm). B/B_m is obtained from Eq. (2.7). Near the circled "magic" ω, B/B_m diverges, so magic trapping is impossible.

Since it is impossible to build a "magic" three-level trap with the alkalis, we need a different atom. Alkaline-earth atoms are a popular choice for many cold-atom trapping experiments, but they have $J = 0$ ground states (zero electronic angular momentum). This means they have no hyperfine structure, and thus no states in which to store qubits.

Instead, we turn to ^{27}Al. It has been successfully laser cooled [14], and as was shown in [3], "magic" trapping of its ground state hyperfine sublevels is aided by comparatively large tensor polarizabilities. This is because the ground state $3p_{1/2}$ is part of a fine-structure multiplet ($3p_{1/2}$ and $3p_{3/2}$): the presence of this nearby state leads to terms with small energy denominators in the perturbation theory expressions for α, but due to angular selection rules these terms enhance only α^T and not α^S.

3.2 Al

Al has only one stable isotope, ^{27}Al, with $I = 5/2$. We consider the $|F' = 3, M_{F'} = 1\rangle$ and $|F = 2, M_F = -1\rangle$ qubit states attached to the $3p_{1/2}$ electronic ground state. The hyperfine splitting is 1.506 GHz, and Eq. (2.6) gives $B_m \approx 4.32$ G. We may use either a linearly or circularly polarized trapping laser.

In the case of a linearly polarized trap, the situation is just as above and similar to that in [16]. The "magic" wavelength is set at $\alpha_{Ryd} = \alpha^S_{3p_{1/2}}$, near $\omega = 0.121$ a.u. ($\lambda = 377$ nm). The large tensor polarizability virtually guarantees that the qubit transition can be made "magic" with a suitable angle choice. Our numerical calculations show the "magic" angle is $\theta_p \approx 65°$.

For a circularly polarized trap, B/B_m remains finite near the "magic" frequency ω_m. The "magic" condition is more complicated, as the ground state second order $\alpha^a_{3p_{1/2}}$ cannot be neglected compared with $\alpha^S_{3p_{1/2}}$. We find the total second-order

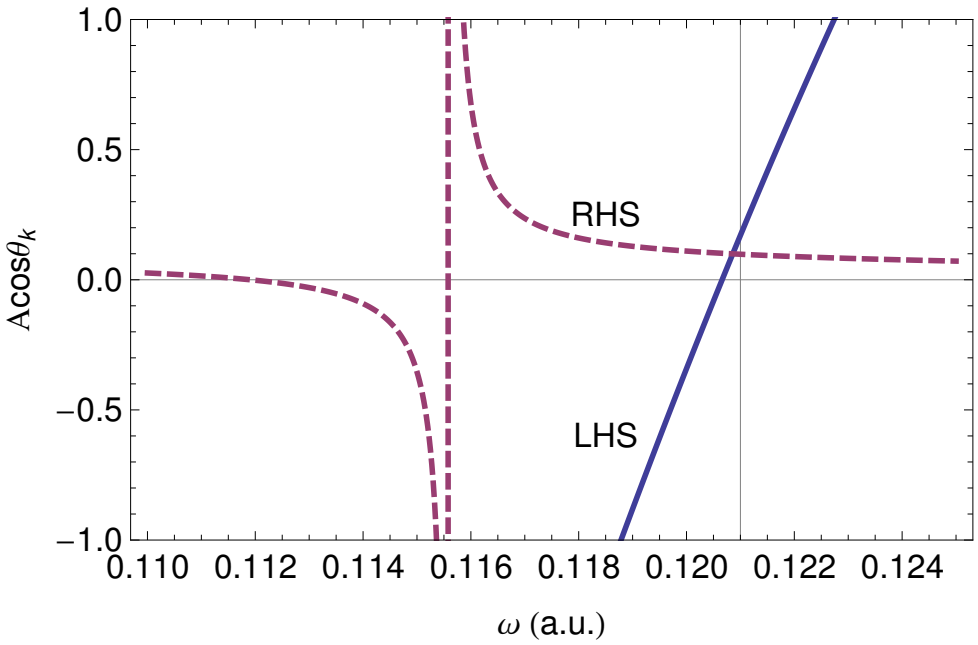

Figure 3.2: (Color online) Left-hand side (solid) and right-hand side (dashed) of Eq. (3.3). "Magic" trapping of the Rydberg transition follows from Eq. (3.2) and lies between the resonance at $\omega = 0.1155$ a.u. ($\lambda = 394$ nm) and the dotted line at $\omega = 0.121$ a.u. ($\lambda = 377$ nm). The "magic" frequency and "magic" angle for the qubit transition are obtained from the curves intersection, just under $\omega = 0.121$ a.u. This combination of ω_{magic} and θ_{magic} will allow Stark and Zeeman insensitive trapping for the three-level system in Al.

polarizability of the ground state from Eq. (2.5)[1]. Equating with the Rydberg polarizability, we obtain

$$\alpha_F^S(\omega) + \mathcal{A}\,\cos\theta_k \frac{M_F}{2F}\alpha_F^a(\omega) = \alpha_{FM_F}^{Ryd}(\omega). \tag{3.2}$$

We must choose ω and θ_k simultaneously satisfy Eqs. (2.7) and (3.2). Solving for $M_F\mathcal{A}\cos\theta_k$ appearing in Eqs. (2.7) and (3.2) and equating the results giving

$$2F'\frac{\omega^{-2} + \alpha_F^S}{\alpha_F^a} = \frac{\beta_{F'}^s - \beta_F^s + \delta\beta^T}{\frac{1}{2F'}\beta_{F'}^a + \frac{1}{2F}\beta_F^a + g_I\frac{\mu_N}{\mu_B}\frac{B}{B_m}\overline{\alpha}_{np_{1/2}}^a}. \tag{3.3}$$

The left and right hand sides of Eq. (3.3) are plotted in Fig. 3.2. Since they intersect in the range allowed by Eq. (3.2), "magic" trapping for this three-level system in Al is possible. While circularly polarized trapping would be experimentally more complex than the linearly polarized trapping, it has the advantage of less Zeeman sensitivity. This is because the "magic" B-field removes Zeeman effects to second-order, while the linearly polarized trap only removes Zeeman decoherence to first order in the B-field.

3.3 Conclusion and Future Work

We have theoretically demonstrated the feasibility of a simultaneous "magic" trap for a three-level system. Such a trap could dramatically reduce decoherence in Rydberg blockade experiments striving towards quantum computation.

It is worth considering what other atoms might be amenable to this trapping scheme. In Sec. 3.1, we remarked that the alkaline-earth atoms could not be trapped with this scheme because they lack hyperfine structure. This is true of their ground

[1] α^T is identically zero as $J = 1/2$.

states. But instead consider a metastable excited state with nonzero J. In particular, we have in mind the lowest $^3P_2$ state, which has a lifetime on the order of seconds. We predict that "magic" trapping would be aided by the nearby fine-structue levels, as we found in Al. "Magic" trapping of the Rydberg states would be aided by the existence of $J = 0$ levels which would be virtually impervious to Zeeman decoherence. Work is currently underway to extend our codes to such divalent systems.

Appendix A

Numerical methods for atomic structure calculations

Our library of codes begins with the B-spline technique to generate a quasi-complete set of orbitals that are solutions to the Dirac-Hartree-Fock equations. To refine these solutions, we find the second-order self-energy operator to build the so-called Brueckner orbitals. Matrix elements are then calculated using the relativistic random-phase approximation. The spline codes are presented in [2], and the other codes are demonstrated in [16].

For this thesis, the new additions to our codes concerned the Rydberg states. To generate a complete B-spline basis set including physically accurate Rydberg states, we radically increased the size of the cavity and the number of basis functions. As an illustration, a typical run to calculate low-lying states uses $\sim$ 40 splines in a $\sim 50a_B$ cavity. For calculations aimed at the $50s$ state, we obtained accurate results using $\sim$ 200 splines in a $\sim 8000a_B$ cavity. We also used a logarithmic rather than an exponential distribution of spline knots. This increased the accuracy of matrix elements by improving the representation of wavefunctions at large R near the cavity wall.

Correlations were included for Rydberg states by building the self-energy operator using a small basis set (~ 40 splines in a $\sim 50a_B$ cavity) and using this potential to build Brueckner orbitals for a large set. This is justified since the self-energy operator diminishes rapidly outside the core, so highly excited states have a negligible contribution. Neglecting these states decreases calculation time dramatically. Inclusion of correlations introduced small but detectable corrections to Rydberg state energies and matrix elements. Corrections were around the fourth significant figure for $n = 50$ states and diminished with increasing n.

References

[1] K. Beloy. PhD Dissertation, University of Nevada, Reno. 2009.

[2] K. Beloy and a. Derevianko. Application of the dual-kinetic-balance sets in the relativistic many-body problem of atomic structure. *Computer Physics Communications*, 179(5):310–319, Sept. 2008.

[3] K. Beloy, A. Derevianko, V. A. Dzuba, and V. V. Flambaum. Micromagic Clock: Microwave Clock Based on Atoms in an Engineered Optical Lattice. *Phys. Rev. Lett.*, 102(12):120801, Mar. 2009.

[4] A. M. Childs and W. van Dam. Quantum algorithms for algebraic problems. *Rev. Mod. Phys.*, 82(1):1–52, Jan. 2010.

[5] J. Clarke and F. K. Wilhelm. Superconducting quantum bits. *Nature*, 453(7198):1031–42, June 2008.

[6] A. Derevianko. "Doubly Magic Conditions in Magic-Wavelength Trapping of Ultracold Alkali-Metal Atoms. *Phys. Rev. Lett.*, 105(3):033002, July 2010.

[7] D. Deutsch. Quantum theory, the Church-Turing principle and the universal quantum computer. *Proc. R. Soc. Lond. A*, 400(1818):97–117, 1985.

[8] D. P. DiVincenzo. The Physical Implementation of Quantum Computation. arXiv::quant–ph/0002077v3, 2008.

[9] R. P. Feynman. Simulating physics with computers. *International Journal of Theoretical Physics*, 21(6-7):467–488, June 1982.

[10] L. Isenhower, W. Williams, A. Dally, and M. Saffman. Atom trapping in an interferometrically generated bottle beam trap. *Opt. Lett.*, 34(8):1159–61, Apr. 2009.

[11] D. Jaksch, J. Cirac, P. Zoller, S. Rolston, R. Côté, and M. Lukin. Fast quantum gates for neutral atoms. *Phys. Rev. Lett.*, 85(10):2208–11, Sept. 2000.

[12] M. D. Lukin, M. Fleischhauer, R. Côté, L. Duan, D. Jaksch, J. Cirac, and P. Zoller. Dipole Blockade and Quantum Information Processing in Mesoscopic Atomic Ensembles. *Phys. Rev. Lett.*, 87(3):037901, June 2001.

[13] N. L. Manakov, V. D. Ovsiannikov, and L. P. Rapoport. Atoms in a laser field. *Phys. Rep.*, 141(6):319–433, Aug. 1986.

[14] R. McGowan, D. Giltner, and S. Lee. Light force cooling, focusing, and nanometer-scale deposition of aluminum atoms. *Opt. Lett.*, 20(24):2535–2537, DEC 15 1995.

[15] J. McKeever, J. R. Buck, a. D. Boozer, a. Kuzmich, H.-C. Nägerl, D. M. Stamper-Kurn, and H. J. Kimble. State-Insensitive Cooling and Trapping of Single Atoms in an Optical Cavity. *Physical Review Letters*, 90(13):2–5, Apr. 2003.

[16] M. J. Morrison, V. A. Dzuba, and A. Derevianko. Possibility of Stark-insensitive cotrapping of two atomic species in optical lattices. *Phys. Rev. A*, 83(1):013604, Jan. 2011.

[17] M. Mosca. Quantum algorithms. arXiv:0808.0369v1, 2008.

[18] R. L. Rivest, A. Shamir, and L. Adleman. A method for obtaining digital signatures and public-key cryptosystems. *Commun. ACM*, 21(2):120–126, Feb. 1978.

[19] P. Rosenbusch, S. Ghezali, V. Dzuba, V. Flambaum, K. Beloy, and A. Derevianko. ac Stark shift of the Cs microwave atomic clock transitions. *Phys. Rev. A*, 79(1):013404, Jan. 2009.

[20] M. Saffman, T. G. Walker, and K. Mø lmer. Quantum information with Rydberg atoms. *Rev. Mod. Phys.*, 82(3):2313–2363, Aug. 2010.

[21] M. Saffman, X. L. Zhang, A. T. Gill, L. Isenhower, and T. G. Walker. Rydberg state mediated quantum gates and entanglement of pairs of neutral atoms. *J. Phys.: Conf. Ser.*, 264:012023, Jan. 2011.

[22] M. S. Safronova, C. J. Williams, and C. W. Clark. Optimizing the fast Rydberg quantum gate. *Phys. Rev. A*, 67(4):040303, Apr. 2003.

[23] P. Shor. Polynomial-time algorithms for prime factorization and discrete logarithms on a quantum computer. *SIAM J. Comput.*, 26(5):1484–1509, 1997.

[24] D. Simon. On the power of quantum computation. *SIAM J. Comput.*, 26(5):1474–1483, 1997.

[25] K. Singer, U. Poschinger, M. Murphy, P. Ivanov, F. Ziesel, T. Calarco, and F. Schmidt-Kaler. Colloquium: Trapped ions as quantum bits: Essential numerical tools. *Reviews of Modern Physics*, 82(3):2609–2632, Sept. 2010.

[26] E. Urban, T. A. Johnson, T. Henage, L. Isenhower, D. D. Yavuz, T. G. Walker, and M. Saffman. Observation of Rydberg blockade between two atoms. *Nature Phys.*, 5(2):110–114, Jan. 2009.

[27] T. G. Walker and M. Saffman. Consequences of Zeeman degeneracy for the van der Waals blockade between Rydberg atoms. *Phys. Rev. A*, 77(3):032723, Mar. 2008.

[28] J. Ye, H. J. Kimble, and H. Katori. Quantum state engineering and precision metrology using state-insensitive light traps. *Science (New York, N.Y.)*, 320(5884):1734–8, June 2008.